

REVIEW

Mitral Regurgitation Evaluation in Modern Echocardiography: Bridging Standard Techniques and Advanced Tools for Enhanced Assessment

Laura Anna Leo  | Giacomo Viani | Susanne Schlossbauer | Sebastiano Bertola | Amabile Valotta | Stephanie Crosio | Matteo Pasini | Alessandro Caretta

Cardiac Imaging Department, Istituto Cardiocentro Ticino, Ente Ospedaliero Cantonale, Lugano, Switzerland

Correspondence: Laura Anna Leo (lauraanna.leo@eoc.ch)

Received: 4 October 2024 | **Revised:** 24 November 2024 | **Accepted:** 1 December 2024

Keywords: advanced echocardiographic tools | mitral valve regurgitation | two- and three-dimensional echocardiography

ABSTRACT

Mitral regurgitation (MR) is one of the most common valvular heart diseases worldwide. Echocardiography remains the first line and most effective imaging modality for the diagnosis of mitral valve (MV) pathology and quantitative assessment of MR. The advent of three-dimensional echocardiography has significantly enhanced the evaluation of MV anatomy and function. Furthermore, recent advancements in cardiovascular imaging software have emerged as step-forward tools, providing a powerful support for acquisition, analysis, and interpretation of cardiac ultrasound images in the context of MR. This review aims to provide an overview of the contemporary workflow for echocardiographic assessment of MR, encompassing standard echocardiographic techniques and the integration of semiautomated and automated ultrasound solutions. These novel approaches include advancements in segmentation, phenotyping, morphological quantification, functional grading, and chamber quantification.

1 | Introduction

Mitral regurgitation (MR) is one of the most common valvular heart diseases worldwide, and its prevalence is expected to increase in the coming decades due to an aging population [1–4]. Patients with symptomatic MR have increased morbidity and mortality if untreated, experiencing poor quality of life and outcomes, even with medical therapy, primarily due to progression to heart failure [5, 6].

1.1 | Classification, Clinical Implications, and Imaging Evaluation of MR

According to etiology, MR can be classified as either primary (degenerative mitral regurgitation [DMR]), a pathological conditions affecting primarily mitral valve (MV) leaflets and/or subvalvular apparatus, or secondary (functional mitral regurgitation [FMR]), related to diseases of the left ventricle (ventricular FMR) or left atrium (atrial FMR). DMR affects about 2%–3% of

Abbreviations: 2DE, 2D echocardiography; 3DE, three-dimensional echocardiography; AI, artificial intelligence; CMR, cardiac magnetic resonance; DL, deep learning; DMR, degenerative mitral regurgitation; EROA, effective regurgitant orifice area; FMR, functional mitral regurgitation; GLS, global longitudinal strain; LA, left atrium; LV, left ventricle; LVEF, left ventricle ejection fraction; MA, mitral annulus; ML, machine learning; MR, mitral regurgitation; MV, mitral valve; RT 3DE, real time three dimensional echocardiography; RVol, regurgitant volume; STE, speckle tracking echocardiography; TEE, transesophageal echocardiography; TTE, transthoracic echocardiography; VC, vena contracta.

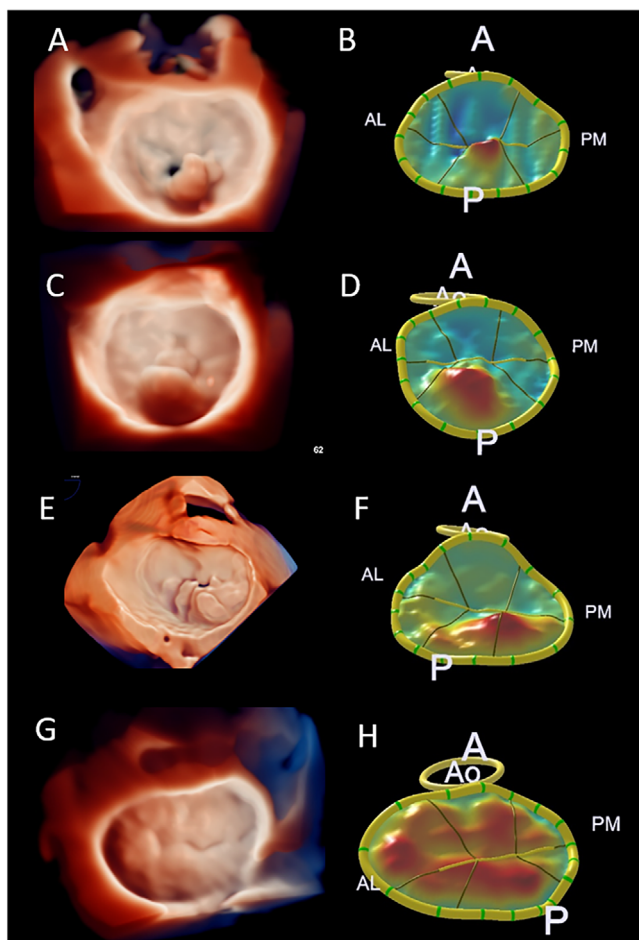


FIGURE 1 | Degenerative mitral regurgitation (DMR) phenotypes in 3D TEE surgical view applying TrueVue transillumination tool (panels A, C, E, G) and surface rendering of MV obtained by computerized modeling of the MV leaflets and annulus (panels B, D, F, H) using MV Navigator AI system. The image shows the spectrum of DMR morphological phenotypes based on the progression of structural abnormalities, described in four main features: (A, B) FED, (C, D) FED+, (E, F) forme fruste, (G, H) Barlow disease. 3D = three-dimensional; AI = artificial intelligence; AML = anterior mitral leaflet; Ao = aortic valve; FED = *fibroelastic deficiency*; FED+ = *fibroelastic deficiency plus*; MV = mitral valve; PML = posterior mitral leaflet; TEE = transoesophageal echocardiography.

the general population and is the leading cause of MV surgery [7]. This lesion corresponds to Carpentier's type II functional classification and encompasses a wide spectrum of morphological phenotypes, based on the progression of valve tissue redundancy: (1) *fibroelastic deficiency* (FED), characterized by a single scallop prolapse or flail with a lack of connective tissue; (2) *fibroelastic deficiency plus* (FED+), a single scallop prolapse with myxomatous degeneration; (3) *forme fruste* (FF), where myxomatous degeneration affects the entire leaflet; and (4) *Barlow disease* (BD), characterized by bileaflets degeneration with multiscalloped prolapse or flail, elongated and thickened chordae tendineae, and annular dilatation [8]. (Figure 1) In contrast, FMR affects up to 24% of patients with systolic heart failure and accounts for 65% of moderate to severe MR cases [9]. No reliable data on the global prevalence of secondary MR are currently available, because its prevalence tends to be underestimated [10]. Ventricular FMR

results from regional or global left ventricular (LV) remodeling, secondary to ischemic or nonischemic cardiomyopathy, leading to papillary muscle displacement, leaflet tethering, and impaired coaptation. It is characterized by an imbalance between *trans*-mitral closure forces and tethering forces, resulting in two distinct patterns: asymmetric and symmetric tethering. This corresponds to Carpentier's type IIIb functional classification [11] (Figure 2). Atrial FMR is related to an isolated left atrium (LA) dilatation due to long-standing atrial fibrillation (AF) and the resulting annular dilatation. It corresponds to Carpentier's type I functional classification [12] (Figure 2).

The underlying mechanism of MR, primary or secondary, defines the therapeutic approach. Accurate assessment of MR severity is crucial for treatment decisions, as both European Society of Cardiology (ESC) and American College of Cardiology/American Heart Association (AHA) guidelines recommend surgery exclusively for patients with severe MR [13, 14]. MR severity is also a key predictor of outcomes in both DMR and FMR, underscoring the clinical importance of precise evaluation and grading [15, 16].

Noninvasive cardiac imaging plays a key role in assessing MR. Echocardiography is the primary imaging tool for evaluating MR mechanism and severity, consequent cardiac remodeling, and prognosis. Two-dimensional (2D) and three-dimensional (3D) transthoracic echocardiography (TTE) are the first-line imaging techniques to assess MR. 2D and 3D transesophageal echocardiography (TEE) are indicated when TTE provides insufficient or inconsistent data for an accurate and complete diagnosis. TEE also plays a crucial role in preprocedural planning and intraoperative guidance [17–20]. Although echocardiography is the main imaging technique for morphological and functional evaluation of MR, cardiac magnetic resonance (CMR) and cardiac computed tomography can complement echocardiography in cases of suboptimal image quality and for preprocedural screening [21–27]. Despite the availability of several guidelines for the assessment of MR, the morphological and functional quantification of MR by echocardiography remains challenging in some cases and is susceptible to significant interobserver variability in its interpretation.

1.2 | Integration of Emerging Advanced Echocardiographic Tools

In recent years, the integration of artificial intelligence (AI) solutions in cardiovascular imaging has emerged as a significant advancement, providing a powerful support for acquisition, analysis, and interpretation of cardiac ultrasound images. AI encompasses computing techniques that simulate logical reasoning, including machine learning (ML) and deep learning (DL). ML is a subset of AI and refers to computational algorithms trained to learn, perform tasks, or make decisions automatically based on available data. DL is a special type of ML that mimics the learning process of the human brain by using artificial neural networks. The most widely implemented model used for cardiac imaging is the convolutional neural network (CNN). DL models, particularly CNNs, excel at automatically encoding features from imaging data, often uncovering insights beyond human interpretation [28–30]. In valvular heart disease, as in MR, AI algorithms focus on images acquisition, segmentation, and

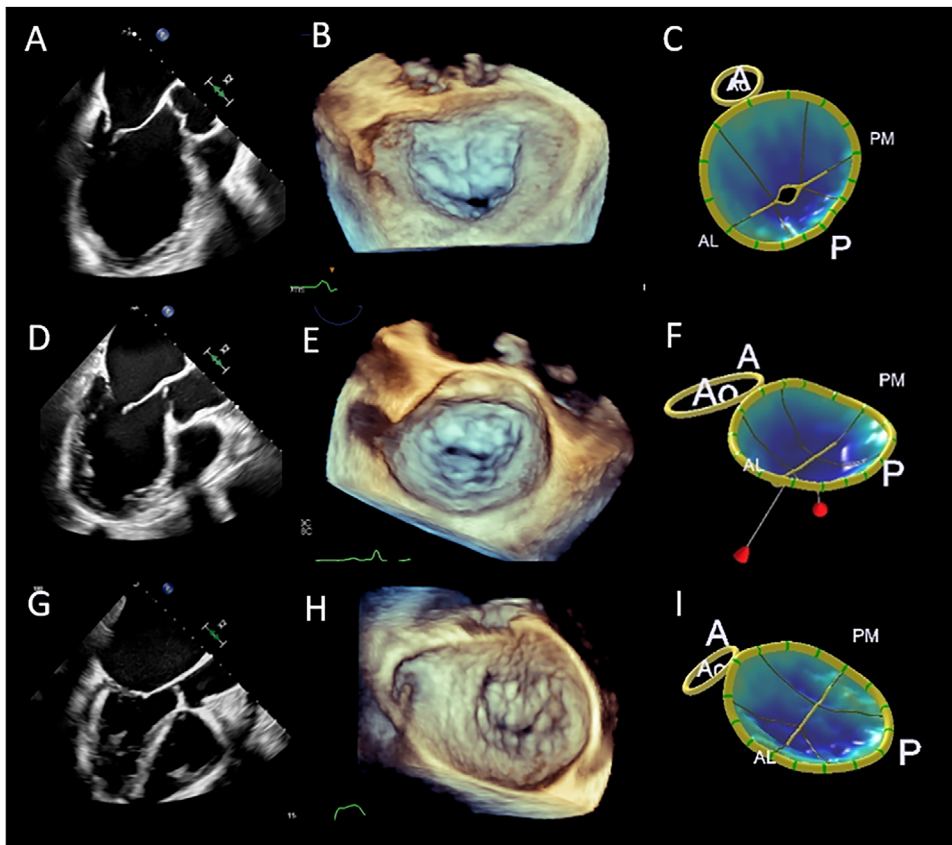


FIGURE 2 | Functional mitral regurgitation (FMR) phenotypes in 2D TEE mid esophageal long axis view (panels A, D, G), 3D TEE Zoom modality in surgical view (panels B, E, H) and surface rendering of mitral valve obtained by computerized modeling of the MV leaflets and annulus (panels C, F, I) using MV Navigator AI system. The image shows the main phenotypes of FMR: (A–C) ventricular asymmetric FMR, (D–F) ventricular symmetric FMR, (G–I) atrial FMR. 2D = two-dimensional; 3D = three-dimensional; AI = artificial intelligence; AML = anterior mitral leaflet; Ao = aortic valve; MV = mitral valve; PML = posterior mitral leaflet; TEE = transoesophageal echocardiography.

quantification of cardiac function and structures to assess valve disease severity and identify high-risk populations [31]. Several AI-enabled echocardiographic solutions—both commercial and noncommercial—have been developed to automate measurements from 2D and 3D images in MV disease. However, the term AI is sometimes overused, considering that early AI applications were often based on computational methods, where mathematical rules are applied for automation, rather than on more specific AI methods such as CNNs. Although some commercial available software are technically semiautomated processes that require initialization by an experienced operator, emerging unsupervised ML and DL approaches with CNN methods are developed or under investigation in the settings of MR. These solutions are increasingly enabling automated screening and stratification of MR severity [32–41]. Nevertheless, AI solutions are not without their limitations. Indeed, their performance is highly dependent on image quality, which can be affected by artifacts, poor resolution, or operator-dependent factors during image acquisition. Moreover, the “black box” nature of many AI systems, particularly those based on DL models, limits interpretability and raises concerns about reliability and confidence among clinicians. Despite these challenges, the integration of AI solutions with clinical expertise provides a pathway to enhance diagnostic accuracy, improve reproducibility and standardization of echocardiographic measurements, and streamline workflows [42–47].

This review aims to present an overview of the contemporary workflow for echocardiographic assessment of MR, incorporating standard echocardiographic techniques alongside the integration of semiautomated and automated ultrasound solutions for segmentation, phenotyping, morphological quantification, functional grading, and chamber quantification.

2 | Segmentation, Phenotyping, and Morphological Quantification of Mitral Valve in MR

The morphological evaluation and quantification of the MV apparatus are of paramount importance for the diagnosis, treatment, and follow-up of patients with MR. Echocardiography is the standard imaging modality used to evaluate MV morphology. The advent of 3D echocardiography (3DE) has significantly enhanced the understanding of MV anatomy and function, with its unique ability to display the MV “en face” in the beating heart, both from atrial and ventricular perspectives. This enables a more accurate morphological and quantitative assessment compared to 2D acquisitions [13, 14, 17, 20, 21].

Many studies have demonstrated the superiority of 3DE over 2D echocardiography (2DE) for visualizing MV morphology, making 3DE the most useful imaging modality for diagnosing MV diseases [48]. 3DE has become the standard imaging modality

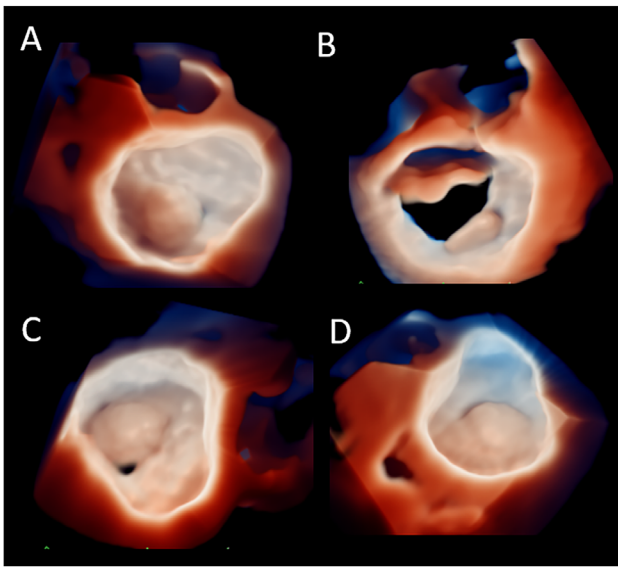


FIGURE 3 | 3D TEE TrueVue zoom modality of MV prolapse shown from multiple perspectives: overhead perspective or surgical view (A), ventricular perspective (B), lateral (C), and medial (D) perspectives. The angled perspectives provide further details of the MV prolapse. 3D = three-dimensional; MV = mitral valve; TEE = transoesophageal echocardiography.

for preoperative assessment and for guiding MV surgery and catheter-based interventions [20, 49]. Different 3DE data acquisition modalities are available, including real-time 3DE (RT 3DE) and ECG-triggered 3DE (zoom and full volume mode, both single and multibeats). The multibeat 3D zoom modality, which provides the highest temporal and spatial resolution, is the preferred mode of acquisition for studying MV anatomy and function.

3D volumetric datasets offer the opportunity to visualize the MV from any angle and perspective [50]. The so-called “surgical view,” which presents an “en face” view of the valve from the atrial perspective, is almost identical to the view observed in the operating room. “Non-surgical views”, and particularly the so-called “angled or tangential views”, provide further details of the MV morphology [51] (Figure 3). Accurate segmentation of the MV and identification of its components, such as the mitral annulus (MA) and leaflets, can support MR diagnosis by providing accurate and quantitative measurements of the anatomy of the regurgitant MV through 3D-guided 2D slices, using multiplanar reconstruction (MPR).

Currently, several commercially available 3DE software solutions provide a detailed, high-resolution reconstruction of the MV. Within these applications, however, AI plays a different role, with earlier versions being semiautomatic, and newer tools incorporating more automated and dynamic features where AI plays a key role. Among the semiautomated tools, for instance, the Mitral Valve Navigator (MVN) (Philips Ultrasound) provides a workflow-driven tool for performing shape analysis on the MV by manually tracking the annulus and leaflets in a single frame on 2D slices derived from a 3D dataset of MV. The 3D parametric map, generated from MV quantification, shows a color-coded topographic display. The newest 3D Auto MV (Philips Ultrasound) offers automated alignment and initialization proposals,

facilitating the workflow and enabling both static and dynamic analyses. Advanced edit options allow for better definition of MV structures, such as leaflet contours, and quantification of the open coaptation area. At the end of the analysis, the MV anatomy and surface are visualized as static and dynamic models. Compared to MVN, 3D Auto MV enables faster and more reproducible analysis thanks to the application of automated algorithms. Both software tools provide several geometric measurements of the MV, such as annular dimensions, leaflet morphology, coaptation description, and relationship between MV and papillary muscles.

3D MV quantification, applying these tools, overcomes the limitations of qualitative interpretation, and improve accuracy, reliability, and interobserver variability, especially among less experienced readers. Even though MR severity assessment is mainly based on the quantitative analysis of regurgitation, quantitative morphological analysis of the MV plays a central role in interventional planning. It facilitates the communication of findings to the interventional team and allows for an individualized interventional approach thereby improving procedural success [52, 53].

In DMR, the use of 3D color-coded parametric models enables direct quantitative analysis on the 3D images proving several measurements such as diameters, circumference and area of the annulus, the annular nonplanarity angle, the aortic-to-MV annulus angle, surface areas and heights of the leaflets, as well as the total and per scallop prolapsing volumes and heights (Figure 4A). By offering these detailed information, accuracy in identifying the site and extent of MV lesions is significantly increased. Quantitative 3D echo analysis enables differentiation of degenerative disease from normal valves based on a billowing height of >1.0 mm. Moreover, a cutoff value of a prolapsing volume of 1.15 mL distinguishes between FED and BD [54]. Quantification analysis in Barlow disease reveals multiscallop prolapse associated with tissue redundancy, larger leaflet areas, greater MA dimensions with increased ellipticity, and flattening, making MA less capable of maintaining leaflet coaptation [55, 56]. The severity of regurgitation in a prolapsing valve correlates with 3DE quantification parameters such as annulus area, leaflet-to-annulus area ratio, leaflet prolapsing volume and height, papillary muscle-to-coaptation length, and annulus saddle-shape flattening (reduced annulus height-to-commissural diameter ratio). An annular height-to-width ratio (AHCWR) of <15% is strongly associated with moderate or severe MR among patients with MV prolapse [57].

In addition to these parameters, 3D TEE and MV quantification in DMR allow for better distinction between clefts (defined as extending $\geq 50\%$ of leaflet height up to the hinge line, dividing a scallop into two parts and causing regurgitation) and indentations. It is important to note that while surgical inspection remains the gold standard, some lesions near the prolapsing leaflet seen on 3DE may not be properly recognized during surgical inspection of a nonbeating heart. Therefore, a topographic map of these lesions may also help in planning the most appropriate interventional approach [58–60].

In FMR, the severity of regurgitation and the indication for revascularization are the main interventional determinants. Nevertheless, quantitative morphological analysis is used to describe the MV in secondary MR (Figure 4B). In ventricular FMR,

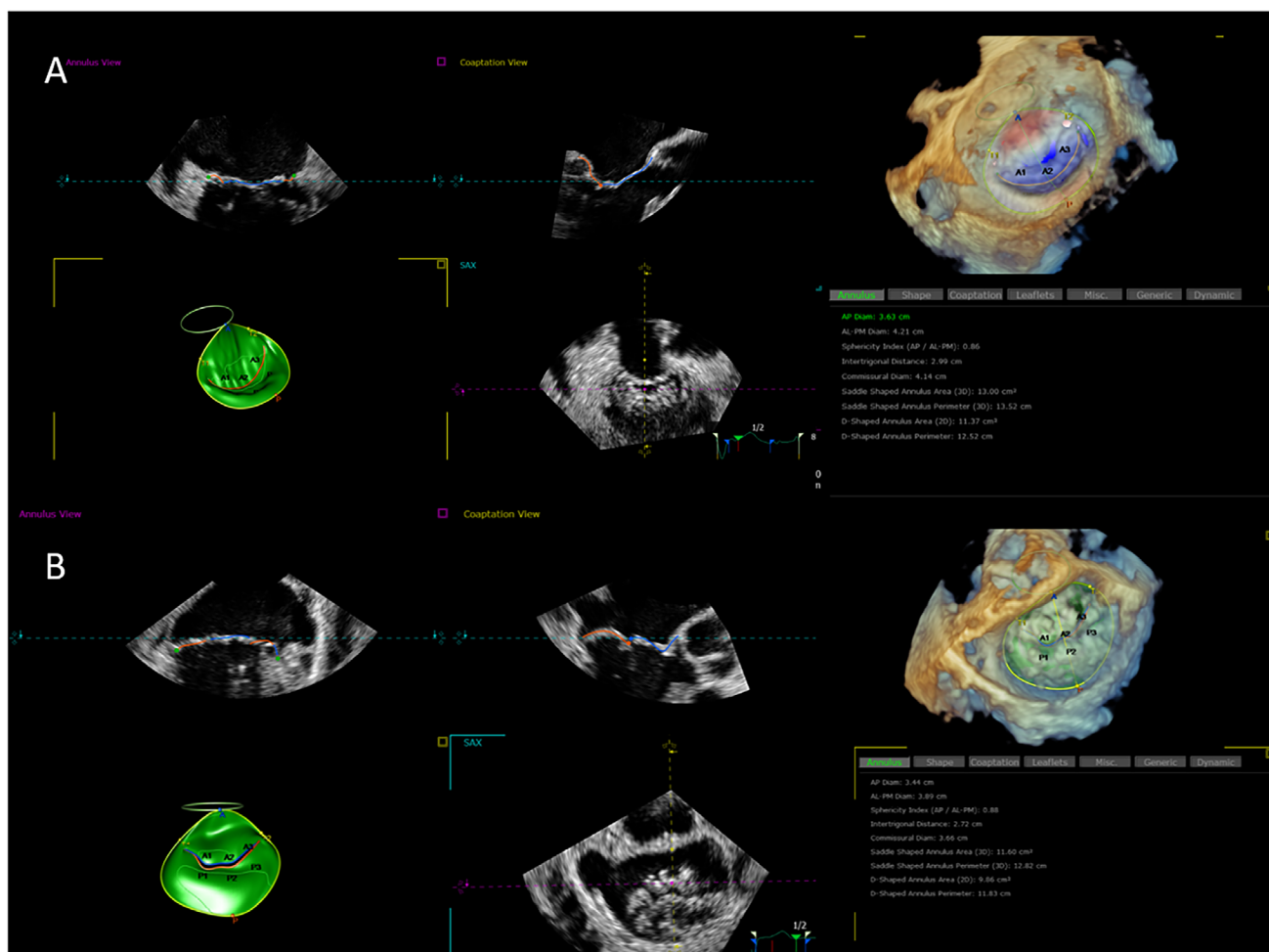


FIGURE 4 | 3D quantitative analysis in degenerative MR (Barlow disease) (panel A) and functional MR (panel B) by 3D Auto MV segmentation. The leaflets and the annulus are automatically tracked in cut planes in a first step within a set frame generating a static model of MV; in a second step of the analysis the tracking is extended over all systolic frames thus providing a dynamic model of MV; in both steps the user has the possibility to edit the automated model proposal. The resulting mitral valve model provides a color-coded surface rendering model of MV together with 3D volume rendering and several automatic quantitative measurements for annulus, leaflets, and coaptation. 3D = three-dimensional; MR, mitral regurgitation; MV = mitral valve.

leaflet tethering occurs due to LV remodeling and papillary muscle displacement, leading to symmetric (predominantly apical tethering of both leaflets) or asymmetric (predominantly posterior tethering) patterns [11]. In atrial FMR, left atrial (LA) enlargement displaces the hinge line of the posterior leaflet over the crest of the LV myocardium, increasing the annulus-papillary distance, thus resulting in a lack of leaflet coaptation [12].

3D quantitative analysis in FMR describes tethering by tenting volume, area, and height (or coaptation depth). The analysis also reveals the enlargement of leaflet surface area as a mechanism of adaptation to chronic LV or LA remodeling. Indeed histological examination of the tethered leaflets provided evidence of active MV leaflet growth through endothelial-mesenchymal differentiation, associated with increased leaflet collagen and thickness, which is independently associated with significant MR [61–63]. In addition, RT 3DE with quantitative analysis of mitral annular dynamics shows that the annulus in ischemic MR is “stiffer” during systole compared to normal MV and degenerative MV disease [64].

3 | Quantification and Grading of Mitral Regurgitation

Accurate quantification of MR severity is crucial for predicting outcomes and guiding treatment decisions, regardless of whether the MR is of primary or secondary etiology. 2D Doppler echocardiography, either transthoracic or transesophageal, is the first-line tool for MR grading. Several qualitative, semiquantitative, and quantitative echocardiographic methods have been proposed [21–65], with current guidelines recommending an integrated approach for the echocardiographic grading of MR severity [13, 14].

Qualitative methods include the visual assessment of continuous wave Doppler intensity and MR jet density, which, when increased, correlate with more severe MR.

Semiquantitative methods rely on: (1) color flow Doppler imaging evaluation of the jet extension into the LA (with a ratio of MR jet area to LA area $\geq 40\%$ indicating severe MR) [66]; (2) the

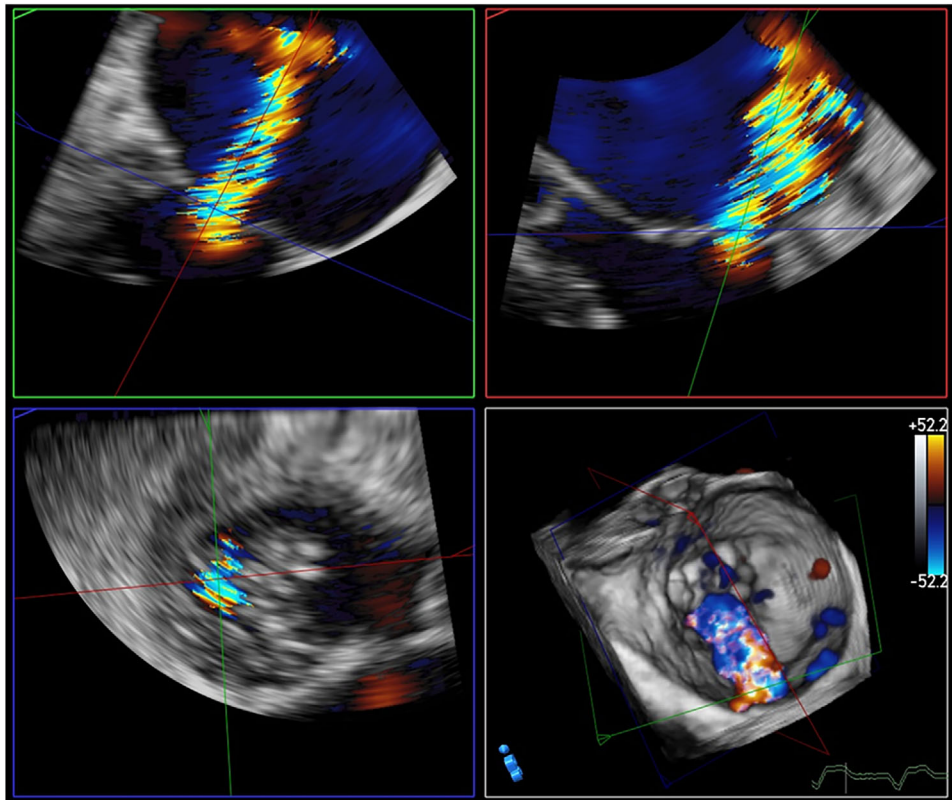


FIGURE 5 | 3D Echocardiographic Technique for the assessment of vena contracta area (EROA-3D). The method uses 2D multiplanar reconstruction derived from a 3D volumetric data set (D) by first positioning two orthogonal image planes along the major axis of the regurgitating jet and then by cropping the 3D data set by a third plane perpendicularly oriented to the jet direction up to the narrowest cross-sectional area of the jet, visualizing 3D VCA (A–C). The EROA-3D is measured by manual planimetry of the color Doppler signal. The image shows an example of EROA-3D assessment in an asymmetric severe functional mitral regurgitation (MR). 2D = two-dimensional; 3D = three-dimensional; 3D VCA = vena contracta area with 3D TEE; TEE = transoesophageal echocardiography.

antegrade velocity of mitral inflow and the pulsed Doppler mitral-to-aortic VTI ratio (peak *E* velocity >1.2 m/s and VTI ratio >1.4 suggest severe MR) [67]; (3) the pulsed Doppler evaluation of pulmonary venous flow patterns (systolic pulmonary flow reversal is specific for severe MR); and (4) the measurement of the vena contracta (VC) width [68]. A VC width ≥ 7 mm defines severe MR.

The most important echocardiographic MR quantitative method is the flow convergence method, with the calculation of effective regurgitant orifice area (EROA) and regurgitant volume (RVol) derived from the proximal isovelocity surface area (PISA) method [21, 65, 69]. An RVol >60 mL and an EROA >40 mm² define severe MR, although in FMR a lower thresholds with a significant impact on outcomes may be applied (EROA >30 mm² and/or RVol >45 mL), especially in elliptical regurgitant orifice or in low-flow conditions [21].

Despite its widespread use, 2D quantification of MR, based on 2D VC and EROA, faces several limitations due to underlying geometrical assumptions. Indeed, the concept of VC assumes that the regurgitant orifice is circular. Whereas the 2D PISA method assumes a hemispheric and symmetric flow convergence area or a single-orifice status. In contrast, the PISA geometry may vary depending on the geometry of the regurgitant orifice and MV leaflets surrounding the orifice. For instance, in FMR

the regurgitant orifice is more elliptical than spherical, thus the 2D PISA method can subsequently underestimate EROA [70]. Moreover, an additional limitation is related to the minimal integration of frame-by-frame or beat-to-beat variability of MR, resulting in challenging quantification in the presence of temporal flow changes of MR, such as in mid- and late-systolic jets, which occur frequently in the presence of MV prolapse [65]. Finally, there is currently no validated approach for the quantification of MR in the presence of multiple jets [65]. Therefore, 2D standard quantification of MR has some important intrinsic limitations, particularly affecting the quantification of multiple, eccentric, and nonholosystolic jets, with suboptimal interobserver agreement.

Recent advancements in automated and semiautomated tools have aimed to address these limitations. Automatic integrated PISA measurements based on the DL algorithm have been proposed for segmentation of the flow convergence region and quantification of MR jet area from 2D color Doppler [71–74]. Recently a novel DL framework, EasyPISA, has been developed for automatic segmentation of the flow convergence region in 2D color Doppler images, without relying on hemispherical assumptions. This method estimates flow rate curves and RVol calculations for all heart cycles, showing a good agreement with manual echocardiographic and CMR imaging assessment of MR severity [39].

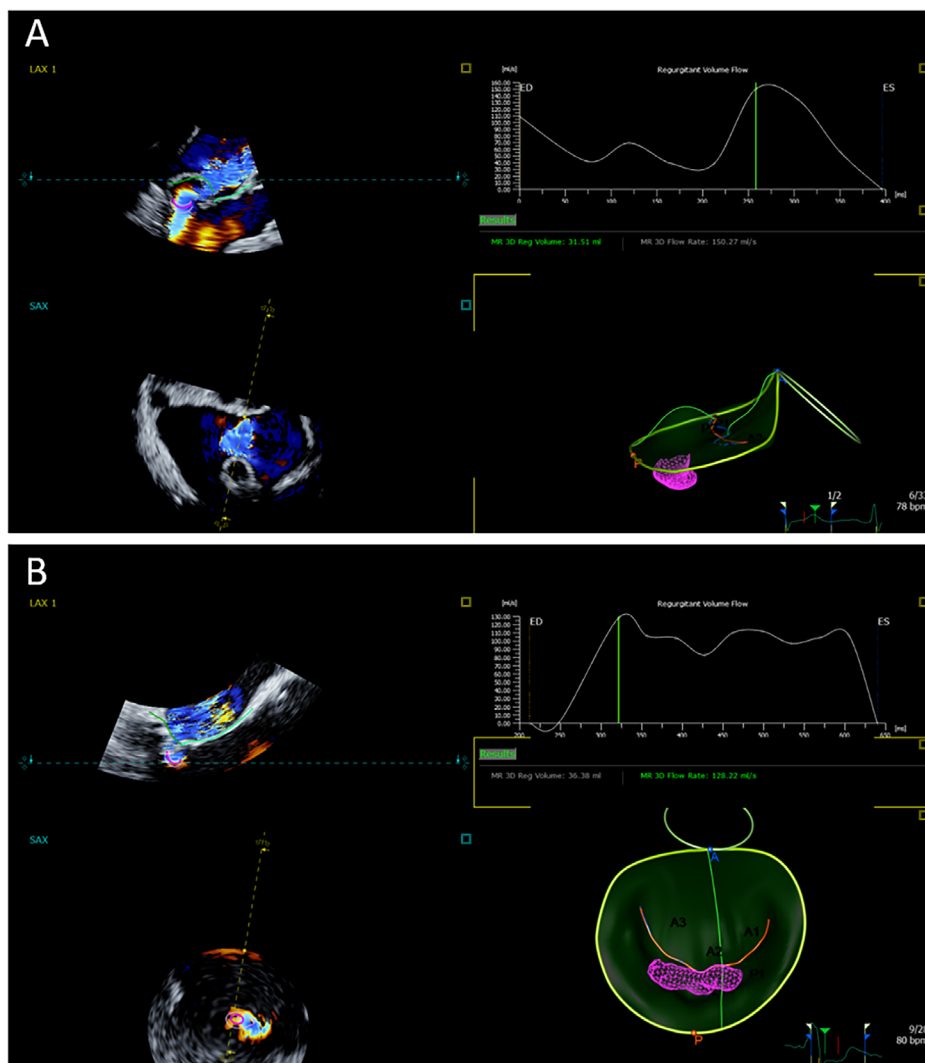


FIGURE 6 | 3D MR flow quantification analysis provided by automatic regurgitant volume analysis AI empowered tool (3D Auto CFQ, Philips) in a case of mitral valve prolapse (panel A) and a case of asymmetric FMR (panel B). 3D analysis runs by detecting the valve morphology from a 3D color Doppler TEE data set on regurgitant MV and then assessing orifice shape, number, and position by using the intersection of color flow Doppler signal and MV surface. By a vector flow fields calculation, the system generates a model of the convergence zone (s), displayed as a purple mesh, and provides measurements of mitral valve regurgitant volume (MV RVol), peak flow rate, and MR dynamic flow curves throughout systole. 3D = three-dimensional; AI = artificial intelligence; FMR = functional mitral regurgitation; MV = mitral valve; PML = posterior mitral leaflet; RVol = regurgitant volume; TEE = transoesophageal echocardiography.

3D color Doppler imaging provides significant advantages over 2D methods by overcoming geometric assumptions. 3D TEE is recommended over 3D TTE because it provides color Doppler images of better quality [17–19].

Measurement of the VC area with 3D TEE (3D VCA) has proven to be more accurate than the 2D VC method for MR quantification, allowing for direct visualization of the orifice morphology [75, 76]. The method uses 2D MPR derived from a 3D volumetric data set by first positioning two orthogonal image planes along the major axis of the regurgitating jet to visualize the jet origin; then, a third perpendicular plane is moved along the length of the jet until its narrowest cross-sectional area is encountered, visualizing 3D VCA. 3D VCA is measured manually by direct planimetry and corresponds to the value of 3D EROA [77] (Figure 5). 3D VCA-derived RVol is obtained by multiplying 3D VCA and the velocity–time integral (VTI) of the regurgitant flow by continuous

wave Doppler. Fully automated ML and DL workflow offers the opportunity for automeasurements of the mitral Doppler signal, making the analysis faster and more reproducible, also among operators with different expertise [74, 79]. The 3D VCA area method is applicable in cases of eccentric or multiple MR jets. Its accuracy has been validated against 2D color Doppler and CMR [77–80]. When using the 2D method as the reference standard for MR grading, a cutoff value of 0.41 cm² for 3D VCA showed 82% sensitivity and 97% specificity in distinguishing moderate from severe MR [81]. Recently it has been demonstrated that a 3D VCA of 0.45 cm² showed 90% sensitivity and 87% specificity to define severe MR in MV prolapse [82].

The PISA method's quantification similarly benefits from 3D color Doppler acquisition. 3D color Doppler echocardiography allows more accurate measurements of MR severity by correcting for the intrinsic geometric limitations of the 2D PISA method,

particularly in eccentric jets with asymmetric orifice and multiple jets [54, 83]. Over the last few years, the feasibility of automated or semiautomated 3D PISA detection has been demonstrated, with good accuracy and reproducibility, even if not always clear the role of AI in modeling [84, 85]. 3D PISA quantification requires the acquisition of a 3DE color Doppler image of the MV, optimizing the sector to obtain the highest possible time resolution. By selecting the aliasing velocity and identifying the PISA in the systolic frame with the largest systolic 3D flow convergence area, a segmentation algorithm allows calculation of true 3D-PISA volume without geometric assumptions, and the volume of more than one PISA simultaneously if multiple jets are present. 3DE-derived PISA volume has been shown to be more accurate and reproducible compared to standard 2D TTE, although with an overestimation of the derived 3D RVol over the 2D RVol in cases of asymmetric or eccentric flow convergence regions, using CMR as a reference [86, 87].

Recently, a novel automated 3D MR flow quantification software (3D Auto Color Flow Quantification CFQ; Philips Ultrasound) has been introduced into clinical practice providing further advancements (Figure 6). 3D Auto CFQ uses 3D color rather than 2D to address the spatial complexities of MR. This new algorithm uses a complex fluid dynamics model, rather than a simple hemispheric PISA model. It is therefore suitable for MR quantification of all orifice geometries and of multiple and eccentric jets [88]. Compared with other models for MR evaluation, which are relatively static using a single frame of the flow convergence, this new algorithm addresses the dynamic variability of the regurgitant orifice and the temporal variation of the regurgitation. Indeed the 3D Auto CFQ application has been developed to evaluate the regurgitant flow at every frame in systole to consider the temporal dynamics of MR. The 3D application Auto CFQ takes advantage of the 3D Auto MV autosegmentation technology (Philips 3D Auto MV) to create an accurate and reproducible model of the MV which is then used as input for the 3D Auto CFQ analysis to quantify MR. The 3D analysis runs by detecting the valve position and morphology from a 3D color Doppler TEE images on MV, creating anatomical Static and Dynamic Model to look for the location of the likely orifice. A vector flow field through single or multiple mitral orifices is calculated, representing the sum of all flow vector forces. The analysis takes into account all the velocities within the Doppler volume, so an aliasing velocity analysis is not needed. The vector field is then converted to 3D color data, enabling the definition of the MV orifice(s) and the instantaneous volume flow for each frame. The integral of flow over all frames provides the total 3D RVol as well as MR dynamic flow curves throughout systole (Figure 6). These flow curves demonstrate the phasic dynamic changes of MR related to the underlying etiology of the regurgitation. In degenerative MR cases the maximal peak is in mid-to-late systole, reflecting the exacerbation of the prolapse or flail throughout systole. In contrast, in functional MR the peak is usually bimodal related to the imbalance between tethering forces and closing forces [89–92]. The current 3D MR flow quantification software has been shown to slightly underestimate RVol, particularly when compared to 2D PISA [88]. This apparent limitation could be related to the fact that RVol quantification is performed over the entire cardiac cycle, rather than being based on a single frame as in the 2D PISA method. Therefore, the optimal cutoff value for severe MR when using this tool must be precisely defined and may differ

from those established with other methods. Overall, 3D MR flow quantification has demonstrated reduced inter- and intraobserver variability compared to standard 2D quantification, highlighting how these AI-driven solutions can enhance reproducibility, even among less experienced operators. Furthermore, the method's short postprocessing time, limited to a few minutes, makes it relatively practical for routine clinical use. However, while 3D Auto Color Flow Quantification of the MV could allow more accurate quantification of MR in more challenging cases, such as functional MR, multiple jets, and constrained or incomplete jets, future larger studies are still needed for better validation.

Another alternative quantitative tool for MR quantification, especially when the PISA and VC methods are not accurate or applicable, is the Doppler volumetric method [21]. In this approach, mitral RVol can be calculated as the difference between total LV stroke volume (the product of MA area and mitral inflow TVI) and systemic stroke volume (obtained by multiplying the left ventricular outflow tract diameter [LVOT] by LVOT TVI). LV total stroke volume can also be measured as the difference between 2D left ventricular end-diastolic volume (LVEDV) and end-systolic volume (LVESV). AI-powered software solutions enable automated Doppler measurements and 2D LV volume quantifications. However, the 2D LV quantification method has not been widely adopted in clinical practice due to its high variability and susceptibility to foreshortening and geometric assumptions. Quantitative assessment of MR regurgitation using 3D TTE volumetric LV quantification has shown more reproducible results compared to CMR, by using 3D analysis from dedicated automated quantification software (e.g., HeartModel, Philips Ultrasound) [85, 93–95]. This software automatically identifies the heart chambers and defines the end-diastolic and end-systolic frames using motion analysis, building up the end-diastolic and end-systolic 3D volumes to calculate the stroke volume. As with Doppler quantification, mitral RVol using HeartModel is measured offline by calculating the difference between LV total stroke volume (obtained from 3D HeartModel acquisition) and aortic forward stroke volume. Despite their advantages, these quantitative methods have limitations and should be used only in cases of isolated MR. They are not suitable, for instance, in the presence of significant aortic regurgitation [21].

4 | Chamber Quantification in MR

Characterization of cardiac chamber remodeling is an integral part of a comprehensive MR assessment [13, 14, 21, 93]. In primary MR, LV and LA remodeling result from chronic volume overload due to the regurgitation. Conversely, secondary MR arises from regional or global LV remodeling related to ischemic or nonischemic cardiomyopathy or from LA remodeling and dilation due to chronic AF in atrial functional MR.

Both LV and LA remodeling are strongly associated with patient outcomes and are key determinants of the timing of interventions. In severe DMR, parameters such as a left ventricular ejection fraction (LVEF) <60%, LV end-systolic diameter >40 mm, LA volume index (LAVi) >60 mL/m² or diameter >55 mm, systolic pulmonary arterial pressure >50 mmHg, and AF are linked to worse outcomes and are considered triggers for intervention, regardless of symptoms [13].

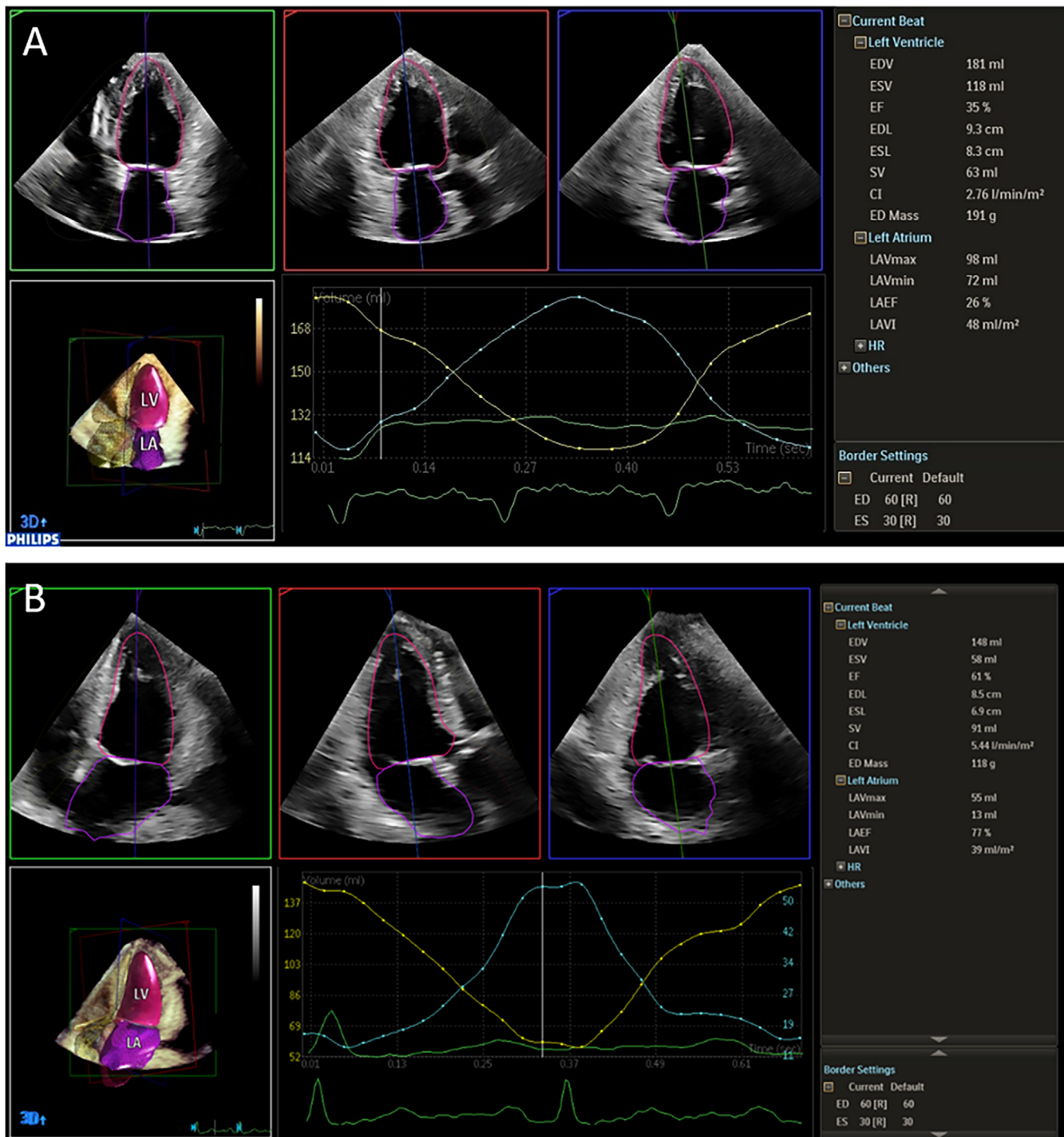


FIGURE 7 | Fully automated left ventricular (LV) and left atrium (LA) analysis by Dynamic HeartModel (DHM, Philips, Amsterdam, the Netherlands). Top panel (A) shows an example of DHM analysis in functional mitral regurgitation (FMR) with reduced ejection fraction (EF) and dilated LA. In the bottom panel (B) a DHM analysis in a DMR with preserved EF and dilated LA.

TTE is the first-line imaging technique for assessing chamber dimensions and function [93]. LV systolic function is traditionally assessed using left ventricle ejection fraction (LVEF), an echocardiographic surrogate for LV contractility, widely accepted for risk stratification and guiding decision-making in clinical practice. For LV volumes and LVEF quantification, both 2D (Simpson's method) and 3D echocardiography are recommended. Although Simpson's method is commonly used, it has notable limitations, including reliance on geometric assumptions, fore-

shortening of the apex, inaccurate border detection, and poor acoustic windows. Three-dimensional echocardiography (3DE), by overcoming these limitations, provides a more accurate evaluation of LV volumes and ejection fraction. Compared to CMR as gold standard, 3DE offers better agreement in LV volume quantification than 2DE [96].

In the last years, AI has emerged as a game-changer in chamber quantification. Several AI automated or semiautomated software

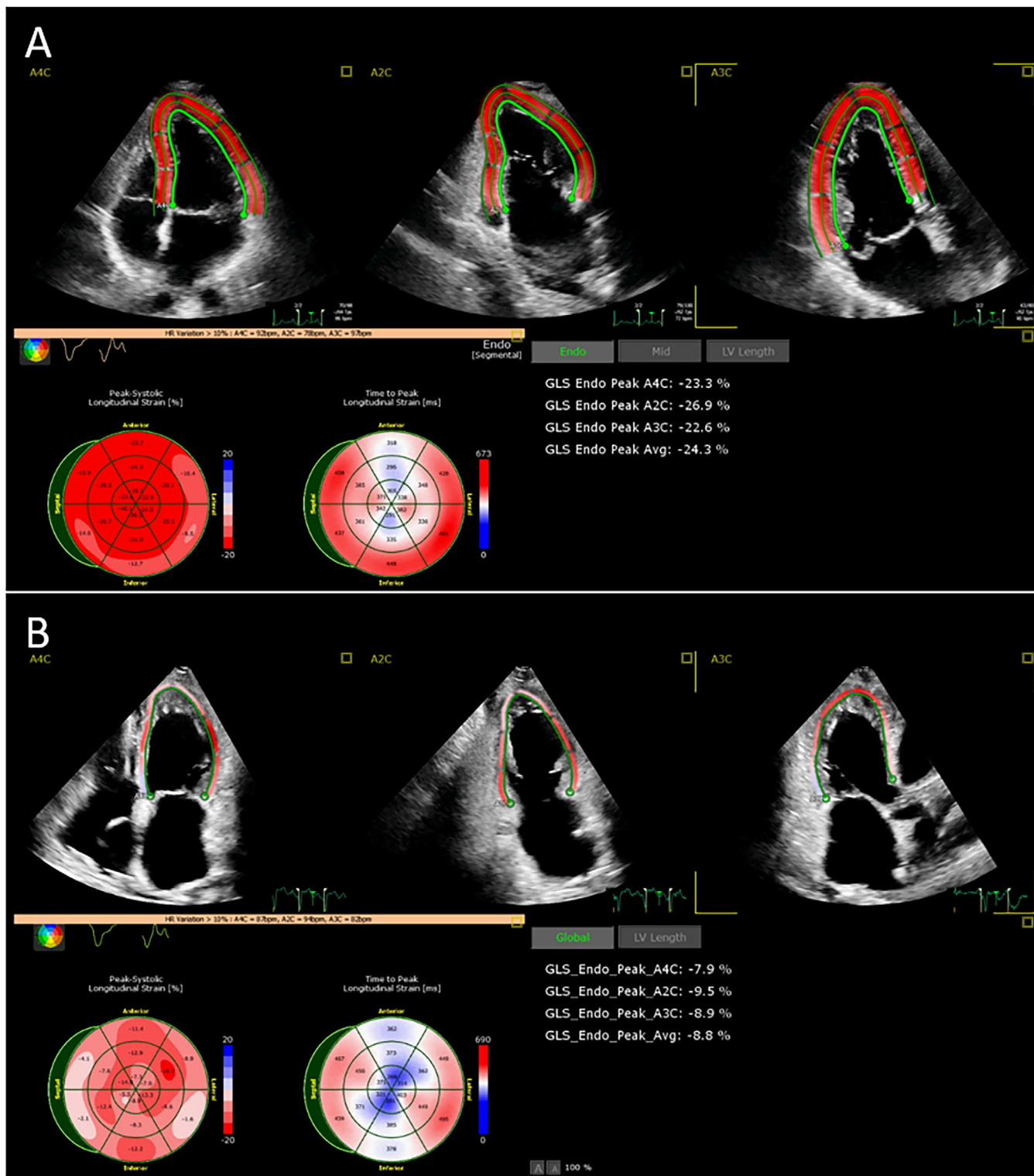


FIGURE 8 | Assessment of left ventricular (LV) global longitudinal strain (GLS) respectively in a patient with mitral valve prolapse and severe mitral regurgitation (panel A) and in a patient with an ischemic severe functional mitral regurgitation (FMR) (panel B). In both cases, a bull's eye plot displays the regional longitudinal strain for each left ventricular segment with a color code. In panel A, GLS is preserved (-24%), whereas in panel B GLS is severely impaired (-8.8%).

tools commercially available offer the opportunity to improve 3D quantitative LV and LA measurements, increasing accuracy and minimizing variability of quantification. Among these tools, the fully automated Dynamic HeartModel A.I. (Philips, Eindhoven, Netherlands) is a model-based segmentation algorithm

that measures the 3D volume of the LV and LA simultaneously from a single 3D acquisition (Figure 7). After acquiring a high-quality TTE 3D volume from the standard apical four-chamber view, including the entire LV and LA, the software tracks the LV and LA borders throughout the cardiac cycle using 3D

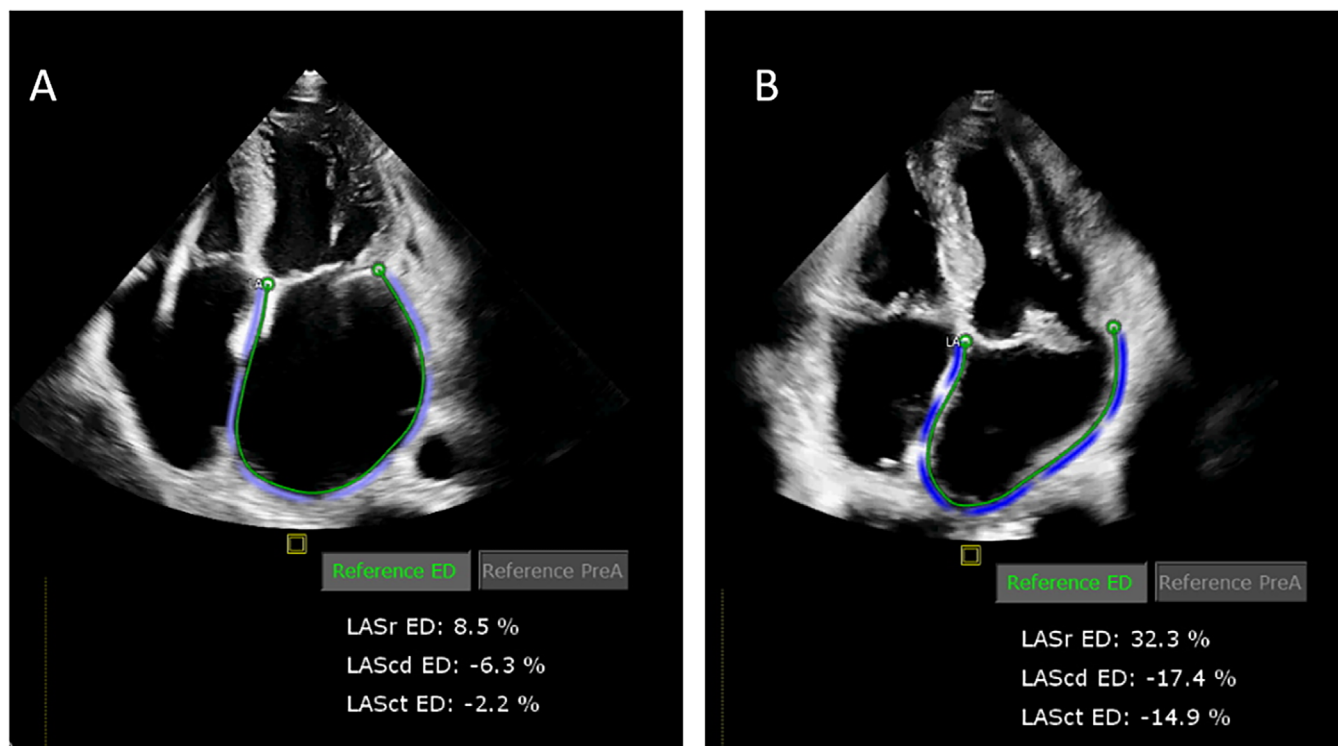


FIGURE 9 | Measurement of atrial longitudinal strain using the speckle tracking echocardiography from an apical 4-chamber view in (A) an atrial FMR and (B) a Barlow disease. FMR = functional mitral regurgitation; LASbp = LA strain at contractive phase; LAScd = LA strain at conduit; LASr = LA strain at reservoir.

speckle technology. The algorithm automatically identifies the end-diastolic (ED) and end-systolic (ES) phases of the cardiac cycle, generating casts of the LV and LA cavities, from which LV and LA volumes are derived directly without geometrical assumptions. Manual editing of the LV and LA endocardial contours is possible when needed. This validated 3D tool has shown an excellent agreement with CMR. It provides robust, accurate, and fast 3D LV and LA analysis, improving efficiency and workflow in echocardiography laboratories thus enabling the routine integration of 3DE for LV and LA quantification [93, 96–98]. However, identifying endocardial boundaries remains challenging in cases of suboptimal image quality or artifacts. An ML algorithm has been trained to automatically estimate LVEF using multiple apical two- and four-chamber views without segmentation or volume quantification, effectively mimicking experienced human visual assessment. This ML algorithm has shown feasibility and accuracy comparable to conventional volume-based measurements [99].

Recent evidences suggest that traditional echocardiography parameters may not detect subclinical ventricular dysfunction. Due to hemodynamic alterations, LVEF may fail to reflect true LV systolic function in patients with MV disease and reduced afterload. Speckle tracking echocardiography (STE), particularly global longitudinal strain (GLS), has been proposed as a more sensitive alternative to LVEF for detecting subclinical LV systolic dysfunction. Advanced deformation imaging facilitates early detection of left heart impairment in chronic MR and has demonstrated incremental prognostic value [100–102]. Several studies have shown that a worse baseline GLS value correlates with poorer clinical outcomes in both primary and secondary MR. LV

GLS has also been identified as an independent predictor of all-cause mortality and adverse cardiac events in patients undergoing MR surgery [102–104]. Measuring LV GLS preoperatively can help identify patients at risk of postoperative LV function decline and optimize surgical timing [104]. Conversely, improvements in LV GLS induced by exercise or medication are associated with better clinical outcomes in primary MR [102].

Recent technological advancements have enabled AI-driven tools to improve strain measurement accuracy. Fully automated or semiautomated GLS measurements using ML-based technology are currently feasible and allow for real-time (few seconds of analysis) GLS calculations, increasing efficiency and reproducibility [105] (Figure 8). For example, the fully automated 2D Auto LV software (Philips, Eindhoven, Netherlands) is a tracking system to quantify LVEF and longitudinal strain, able to automatically select optimal images for 2D LV assessment, providing automated 2D strain and LVEF analysis within the same application. This approach improves workflow and ensures reproducible results, although image quality, operator variability, and differences between software platforms can affect strain measurement accuracy [106–109]. Despite these limitations, STE represents a significant advancement over traditional echocardiographic parameters, providing a more accurate and sensitive assessment of cardiac function, which can help identify in an early stage patients at risk of cardiac adverse events.

Strain analysis is valuable for detecting LA dysfunction in MR. Initially, LA dilation compensates the volume overload, but progressive dilation leads to interstitial fibrosis, reduced compliance, and dysfunction [101]. LA function is traditionally

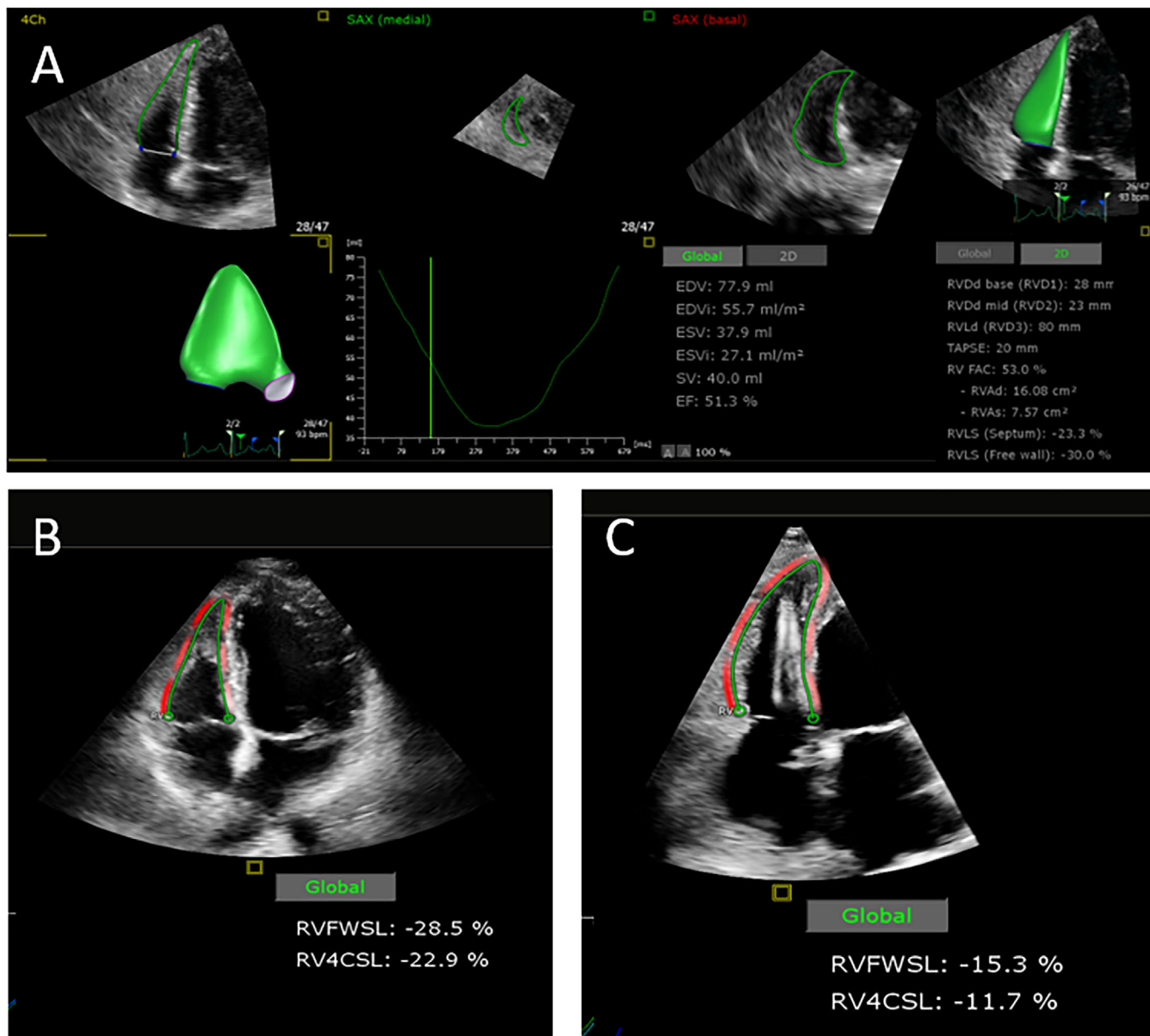


FIGURE 10 | Assessment of right ventricle (RV) dimension and function. (A) 3D Auto RV quantification tool allows 3D RV volumes and ejection fraction quantification alongside 2D parameters. (B, C) Echocardiography-derived right ventricular global longitudinal strain in a patient with DMR with preserved RV function (B) and in a patient with severe functional mitral regurgitation and impaired LV and RV functions (C). 2D = two-dimensional; 3D = three-dimensional; DMR = degenerative mitral regurgitation; RV4CSL = right ventricular global longitudinal strain in 4-chamber view; RVFWS = right ventricular free wall strain.

described by three phases: the reservoir phase (LA filling during LV systole), the conduit phase (passive LV filling during early diastole), and the booster-pump phase (active LA contraction during late diastole). Each of these phases can be analyzed using 2D speckle-tracking echocardiography to assess LA deformation (Figure 9). Peak atrial longitudinal strain (PALS), measured during the reservoir phase, has been reported as a sensitive marker of LA function, capable of identifying atrial dysfunction in the early stages, even before LA dilation occurs [110]. Several studies have shown a strong correlation between atrial strain, measured by PALS, and the degree of LA fibrosis, a sign of unfavorable atrial remodeling, and a risk factor for adverse events and AF [111]. Moreover in patients undergoing MV repair for severe primary

MR, LA reservoir strain has been shown to be an independent predictor of all-cause mortality [112].

Finally, right ventricular (RV) dimensions and function assessment is also important in the clinical setting of MR particularly before interventional procedures [113]. Preoperative RV structural and functional impairment is associated with a higher risk of worse postoperative outcomes [114]. In addition to validated 2D parameters recommended for quantifying RV dimension and function (basal and mid-cavity diameters, RV fractional area change, tricuspid annular plane systolic excursion, tricuspid annular systolic tissue Doppler velocity), 3D RV evaluation is currently available overcoming 2D limitations due to the complexity of RV shape and anatomy. The 3D assessment of RV is

based on an ML artificial algorithm, similar to Heart Model, which provides an autosegmentation of RV volume enabling faster and reproducible assessments of RV function and stroke volume (Figure 10A) [115]. Moreover, as with LV evaluation, RV strain has proven to be superior in assessing global RV function, demonstrating strong correlations with RV pressures and outcomes in patients with MR and heart failure [116, 117]. Recently, AI solutions have enabled automated quantification of RV strain, including both RV free wall strain (RVFWS) and right ventricular global longitudinal strain (RVGLS) (Figure 10B, C).

5 | Conclusion

Echocardiography remains the first-line and most useful imaging technique for the diagnosis of MV pathology and for quantitative assessment of MR. The advent of 3D echocardiography, particularly real time 3D TEE, has significantly improved the evaluation of MV anatomy and function, offering distinct advantages over 2DE. In recent years, the integration of automated and semiautomated AI algorithms into routine echocardiographic assessments has further improved MR evaluation. These tools facilitate segmentation, phenotyping, morphological, functional, and chamber quantification. Based on our experiences, the application of these tools provides a valuable support to imagers, bridging the gaps in human expertise and offering deeper insights into MR assessments. This led to more standardized imaging assessments and data collection improving consistency, reproducibility, and workflow efficiency by reducing repetitive tasks. Despite these advancements, AI solutions have limitations, and the operator's expertise remains essential for interpreting complex datasets and integrating AI findings into clinical practice. Looking ahead, the application of DL methods is expected to further refine the classification of MR patients according to etiology, severity, and treatment suitability. These advancements will have significant potential to enhance clinical support in decision-making, optimize treatment strategies, and improve patient outcome.

Ethics Statement

This study was conducted in accordance with the ethical standards of the Declaration of Helsinki and approved by the Institutional Review Board.

Conflicts of Interest

The authors declare no conflicts of interest.

Data Availability Statement

No data were analysed for or in support of this review

References

1. V. T. Nkomo, J. M. Gardin, and T. N. Skelton, "Burden of Valvular Heart Diseases: A Populationbased Study," *Lancet* 368 (2006): 1005–1011.
2. S. Coffey, R. Roberts-Thomson, A. Brown, et al., "Global Epidemiology of Valvular Heart Disease," *Nature Reviews Cardiology* 18 (2021): 853–864.
3. B. Iung, V. Delgado, R. Rosenhek, et al., "Contemporary Presentation and Management of Valvular Heart Disease: The EURObservational Research Programme Valvular Heart Disease II Survey," *Circulation* 140 (2019): 1156–1169.

4. J. L. d'Arcy, S. Coffey, M. A. Loudon, et al., "Large-Scale Community Echocardiographic Screening Reveals a Major Burden of Undiagnosed Valvular Heart Disease in Older People: The OxVALVE Population Cohort Study," *European Heart Journal* 37 (2016): 3515–3522.
5. V. Dziadzko, M. Dziadzko, J. R. Medina-Inojosa, et al., "Causes and Mechanisms of Isolated Mitral Regurgitation in the Community: Clinical Context and Outcome," *European Heart Journal* 40 (2019): 2194–2202.
6. O. Mesi, M. M. Gad, A. D. Crane, et al., "Severe Atrial Functional Mitral Regurgitation: Clinical and Echocardiographic Characteristics, Management and Outcomes," *JACC: Cardiovascular Imaging* 14 (2021): 797–808.
7. L. A. Freed, D. Levy, R. A. Levine, et al., "Prevalence and Clinical Outcome of Mitral Valve Prolapse," *New England Journal of Medicine* 341 (1999): 1–7.
8. D. H. Adams, R. Rosenhek, and V. Falk, "Degenerative Mitral Valve Regurgitation: Best Practice Revolution," *European Heart Journal* 31 (2010): 1958–1966.
9. F. Grigioni, M. Enriquez-Sarano, K. J. Zehr, et al., "Ischemic Mitral Regurgitation: Long-Term Outcome and Prognostic Implications With Quantitative Doppler Assessment," *Circulation* 103 (2001): 1759–1764.
10. B. Iung, and A. Vahanian, "Epidemiology of Valvular Heart Disease in the Adult A," *Nature Reviews Cardiology* 8 (2011): 162–172.
11. E. Agricola, M. Oppizzi, M. Pisani, et al., "Ischemic Mitral Regurgitation: Mechanisms and Echocardiographic Classification," *European Journal of Echocardiography* 9 (2008): 207–221.
12. W. A. Zoghbi, R. A. Levine, F. Flachskampf, et al., "Atrial Functional Mitral Regurgitation," *JACC: Cardiovascular Imaging* 15 (2022): 1870–1882.
13. A. Vahanian, F. Beyersdorf, and F. Praz, "ESC/EACTS Scientific Document Group, ESC National Cardiac Societies, 2021 ESC/EACTS Guidelines for the Management of Valvular Heart Disease: Developed by the Task Force for the Management of Valvular Heart Disease of the European Society of Cardiology (ESC) and the European Association for Cardio-Thoracic Surgery (EACTS)," *European Heart Journal* 43, no. 7 (2022): 561–632.
14. C. M. Otto, R. A. Nishimura, R. O. Bonow, et al., "2020 ACC/AHA Guideline for the Management of Patients with Valvular Heart Disease: Executive Summary: A Report of the American College of Cardiology/American Heart Association Joint Committee on Clinical Practice Guidelines," *Circulation* 143, no. 5 (2021): e35–e71.
15. F. Grigioni, M. Enriquez-Sarano, K. J. Zehr, et al., "Ischemic Mitral 753 Regurgitation: Long Term Outcome and Prognostic Implications With Quantitative Doppler Assessment," *Circulation* 103 (2001): 1759–1764.
16. M. Enriquez-Sarano, J. F. Avierinos, D. Messika-Zeitoun, et al., "Quantitative Determinants of Outcome of Asymptomatic Mitral Regurgitation," *New England Journal of Medicine* 352 (2005): 875–883.
17. R. M. Lang, L. P. Badano, W. Tsang, et al., "EAE/ASE Recommendations for Image Acquisition and Display Using Three-Dimensional Echocardiography," *Journal of the American Society of Echocardiography* 25 (2012): 3–46.
18. R. M. Lang, W. Tsang, L. Weinert, V. Mor-Avi, and S. Chandra, "Valvular Heart Disease. The Value of 3-Dimensional Echocardiography," *Journals of the American College of Cardiology* 58 (2011): 1933–1944.
19. F. F. Faletra, E. Agricola, F. A. Flachskampf, et al., "Three-Dimensional Transoesophageal Echocardiography: How to Use and When to Use—a Clinical Consensus Statement From the European Association of Cardiovascular Imaging of the European Society of Cardiology," *European Heart Journal – Cardiovascular Imaging* 24, no. 8 (2023): e119–e197. Erratum in: *European Heart Journal – Cardiovascular Imaging* 25, no. 2 (2024): e99.
20. F. F. Faletra, A. Berrebi, G. Pedrazzini, et al., "3D transesophageal Echocardiography: A New Imaging Tool for Assessment of Mitral

- Regurgitation and for Guiding Percutaneous Edge-to-Edge Mitral Valve Repair,” *Progress in Cardiovascular Diseases* 60 (2017): 305–321.
21. P. Lancellotti, P. Pibarot, J. Chambers, et al., “Scientific Document Committee of the European Association of Cardiovascular Imaging. Multi-Modality Imaging Assessment of Native Valvular Regurgitation: An EACVI and ESC Council of Valvular Heart Disease Position Paper,” *European Heart Journal – Cardiovascular Imaging* 23, no. 5 (2022): e171–e232.
 22. S. Uretsky, E. Argulian, J. Narula, et al., “Use of Cardiac Magnetic Resonance Imaging in Assessing Mitral Regurgitation: Current Evidence,” *Journal of the American College of Cardiology* 71 (2018): 547–563.
 23. P. Garg, A. J. Swift, L. Zhong, et al., “Assessment of Mitral Valve Regurgitation by Cardiovascular Magnetic Resonance Imaging,” *Nature Reviews Cardiology* 17 (2019): 298–312.
 24. M. W. S. Kon, S. Myerson, N. E. Moat, et al., “Quantification of Regurgitant Fraction in Mitral Regurgitation by Cardiovascular Magnetic Resonance: Comparison of Techniques,” *Journal of Heart Valve Disease* 13 (2004): 600–607.
 25. E. E. Calkoen, A. A. Roest, L. J. Kroft, et al., “Characterization and Improved Quantification of Left Ventricular Inflow Using Streamline Visualization With 4DFlow MRI in Healthy Controls and Patients After Atrioventricular Septal Defect Correction,” *Journal of Magnetic Resonance Imaging* 41 (2014): 1512–1520.
 26. P. Dyverfeldt, M. Bissell, A. J. Barker, et al., “4D Flow Cardiovascular Magnetic Resonance Consensus Statement,” *Journal of Cardiovascular Magnetic Resonance* 17 (2015): 72.
 27. D. E. Litmanovich and J. Kirsch, “Computed Tomography of Cardiac Valves,” *Radiologic Clinics of North America* 57 (2019): 141–164.
 28. A. D. Dey, P. J. Slomka, P. Leeson, et al., “Artificial Intelligence in Cardiovascular Imaging: JACC State-of-the-Art Review,” *Journal of the American College of Cardiology* 73, no. 11 (2019): 1317–1335.
 29. P. Sardar, J. D. Abbott, A. Kundu, et al., “Impact of Artificial Intelligence on Interventional Cardiology: From Decision-Making Aid to Advanced Interventional Procedure Assistance,” *JACC: Cardiovascular Interventions* 12, no. 14 (2019): 1293–1303.
 30. T. Barry, J. M. Farina, C. J. Chao, et al., “The Role of Artificial Intelligence in Echocardiography,” *Journal of Imaging* 9 (2023): 50.
 31. R. Nedadur, B. Wang, and W. Tsang, “Artificial Intelligence for the Echocardiographic Assessment of Valvular Heart Disease,” *Heart* 108 (2022): 1592–1599.
 32. E. Costa, N. Martins, M. S. Sultan, et al., “Mitral Valve Leaflets Segmentation in Echocardiography Using Convolutional Neural Networks,” *IEEE Portuguese Meeting on Bioengineering ENBENG 2019* (2019): 1–4.
 33. B. S. Andreassen, F. Veronesi, O. Gerard, et al., “Mitral Annulus Segmentation Using Deep Learning in 3-D Transesophageal Echocardiography,” *IEEE Journal of Biomedical and Health Informatics* 24 (2020): 994–1003.
 34. L. Corinzia, F. Laumer, A. Candreva, et al., “Neural Collaborative Filtering for Unsupervised Mitral Valve Segmentation in Echocardiography,” *Artificial Intelligence in Medicine* 110 (2020): 101975.
 35. J. A. Naser, E. Lee, S. V. Pislaru, et al., “Artificial Intelligence-Based Classification of Echocardiographic Views,” *European Heart Journal – Digital Health* 5, no. 3 (2024): 260–269.
 36. F. Yang, X. Chen, X. Lin, et al., “Automated Analysis of Doppler Echocardiographic Videos as a Screening Tool for Valvular Heart Diseases,” *JACC: Cardiovascular Imaging* 15, no. 4 (2022): 551–563.
 37. M. Vafaezadeh, H. Behnam, A. Hosseinsabet, et al., “Automatic Morphological Classification of Mitral Valve Diseases in Echocardiographic Images Based on Explainable Deep Learning Methods,” *International Journal for Computer Assisted Radiology and Surgery* 17, no. 2 (2022): 413–425.
 38. S. V. Wifstad, H. A. Kildahl, B. Grenne, et al., “Mitral Valve Segmentation and Tracking From Transthoracic Echocardiography Using Deep Learning,” *Ultrasound in Medicine & Biology* 50, no. 5 (2024): 661–670.
 39. S. V. Wifstad, H. A. Kildahl, E. Holte, et al., “EasyPISA: Automatic Integrated PISA Measurements of Mitral Regurgitation from 2-D Color-Doppler Using Deep Learning,” *Ultrasound in Medicine & Biology* 50, no. 11 (2024): 1628–1637.
 40. A. Vrudhula, G. Duffy, M. Vukadinovic, et al., “High-Throughput Deep Learning Detection of Mitral Regurgitation,” *Circulation* 150, no. 12 (2024): 923–933.
 41. H. Moghaddasi and S. Nourian, “Automatic Assessment of Mitral Regurgitation Severity Based on Extensive Textural Features on 2D Echocardiography Videos,” *Computers in Biology and Medicine* 73 (2016): 47–55.
 42. A. Davis, K. Billick, K. Horton, et al., “Artificial Intelligence and Echocardiography: A Primer for Cardiac Sonographers,” *Journal of the American Society of Echocardiography* 33 (2020): 1061–1066.
 43. A. Sehly, B. Jaltotage, A. He, et al., “Artificial Intelligence in Echocardiography: The Time Is Now,” *Reviews in Cardiovascular Medicine* 23 (2022): 256.
 44. R. Nedadur, B. Wang, and W. Tsang, “Artificial Intelligence for the Echocardiographic Assessment of Valvular Heart Disease,” *Heart* 108 (2022): 1592–1599.
 45. J. Zhou, M. Du, S. Chang, et al., “Artificial Intelligence in Echocardiography: Detection, Functional Evaluation, and Disease Diagnosis,” *Cardiovascular Ultrasound* 19 (2021): 29.
 46. S. Gandhi, W. Mosleh, J. Shen, et al., “Automation, Machine Learning, and Artificial Intelligence in Echocardiography: A Brave New World,” *Echocardiography* 35, no. 9 (2018): 1402–1418.
 47. A. Long, C. M. Haggerty, J. Finer, et al., “Deep Learning for Echo Analysis, Tracking, and Evaluation of Mitral Regurgitation (DELINEATE-MR),” *Circulation* 150 (2024): 911–922.
 48. G. La Canna, I. Arendar, F. Maisano, et al., “Real-Time Three-Dimensional Transesophageal Echocardiography for Assessment of Mitral Valve Functional Anatomy in Patients With Prolapse-Related Regurgitation,” *American Journal of Cardiology* 107 (2011): 1365–1374.
 49. E. Agricola, F. Ancona, T. Bartel, et al., “Multimodality Imaging for Patient Selection, Procedural Guidance, and Follow-Up of Transcatheter Interventions for Structural Heart Disease: A Consensus Document of the EACVI Task Force on Interventional Cardiovascular Imaging: Part 1: Access Routes, Transcatheter Aortic Valve Implantation, and Transcatheter Mitral Valve Interventions,” *European Heart Journal – Cardiovascular Imaging* 24, no. 9 (2023): e209–e268.
 50. F. F. Faletra, S. Demertzis, G. Pedrazzini, et al., “Three-Dimensional Transesophageal Echocardiography in Degenerative Mitral Regurgitation,” *Journal of the American Society of Echocardiography* 28 (2015): 437–448.
 51. P. Biaggi, C. Gruner, S. Jedrzkiewicz, et al., “Assessment of Mitral Valve Prolapse by 3D TEE: Angled Views Are Key,” *JACC: Imaging* 4 (2011): 94–97.
 52. J. Chikwe, D. H. Adams, K. N. Su, et al., “Can Three-dimensional Echocardiography Accurately Predict Complexity of Mitral Valve Repair?” *European Journal of Cardio-Thoracic Surgery* 41 (2012): 518–524.
 53. W. Tsang and R. M. Lang, “Three-Dimensional Echocardiography Is Essential for Intraoperative Assessment of Mitral Regurgitation,” *Circulation* 128, no. 6 (2013): 643–652.
 54. S. Chandra, I. S. Salgo, L. Sugeng, et al., “Characterization of Degenerative Mitral Valve Disease Using Morphologic Analysis of Real-Time Three-Dimensional Echocardiographic Images: Objective Insight Into Complexity and Planning of Mitral Valve Repair,” *Circulation: Cardiovascular Imaging* 4 (2011): 24–32.
 55. F. Maffessanti, N. A. Marsan, G. Tamborini, et al., “Quantitative Analysis of Mitral Valve Apparatus in Mitral Valve Prolapse Before

- and After Annuloplasty: A Three-dimensional Intraoperative Transesophageal Study," *Journal of the American Society of Echocardiography* 24 (2011): 405–413.
56. C. Antoine, F. Mantovani, G. Benfari, et al., "Pathophysiology of Degenerative Mitral Regurgitation: New 3-Dimensional Imaging Insights," *Circulation: Cardiovascular Imaging* 11 (2018): e005971.
57. A. P. Lee, M. C. Hsiung, I. S. Salgo, et al., "Quantitative Analysis of Mitral Valve Morphology in Mitral Valve Prolapse With Real-Time 3-Dimensional Echocardiography: Importance of Annular Saddle Shape in the Pathogenesis of Mitral Regurgitation," *Circulation* 127 (2013): 832–834.
58. X. Yuan, A. Zhou, and L. Chen, "Diagnosis of Mitral Valve Cleft Using Real-Time 3-Dimensional Echocardiography," *Journal of Thoracic Disease* 9 (2017): 159–165.
59. L. Ring, B. S. Rana, S. Y. Ho, et al., "The Prevalence and Impact of Deep Clefts in the Mitral Leaflets in Mitral Valve Prolapse," *European Heart Journal – Cardiovascular Imaging* 14, no. 6 (2013): 595–602.
60. G. La Canna, I. Arendar, F. Maisano, et al., "Real-Time Three-Dimensional Transesophageal Echocardiography for Assessment of Mitral Valve Functional Anatomy in Patients With Prolapse-Related Regurgitation," *American Journal of Cardiology* 107 (2011): 1365–1374.
61. J. P. Dal-Bianco, E. Aikawa, J. Bischoff, et al., "Active Adaptation of the Tethered Mitral Valve: Insights Into a Compensatory Mechanism for Functional Mitral Regurgitation," *Circulation* 120 (2009): 334–342.
62. J. Beaudoin, J. P. Dal-Bianco, E. Aikawa, et al., "Mitral Leaflet Changes Following Myocardial Infarction: Clinical Evidence for Maladaptive Valvular Remodeling," *Circulation: Cardiovascular Imaging* 10, no. 11 (2017): e006512.
63. D. H. Kim, R. Heo, M. D. Handschumacher, et al., "Mitral Valve Adaptation to Isolated Annular Dilation: Insights Into the Mechanism of Atrial Functional Mitral Regurgitation," *JACC: Cardiovascular Imaging* 12 (2019): 665–677.
64. Y. Topilsky, O. Vaturi, N. Watanabe, et al., "Real-Time 3-Dimensional Dynamics of Functional Mitral Regurgitation: A Prospective Quantitative and Mechanistic Study," *Journal of the American Heart Association* 2 (2013): e000039.
65. W. A. Zoghbi, D. Adams, R. O. Bonow, et al., "Recommendations for Noninvasive Evaluation of Native Valvular Regurgitation: A Report From the American Society of Echocardiography Developed in Collaboration With the Society for Cardiovascular Magnetic Resonance," *Journal of the American Society of Echocardiography* 30, no. 4 (2017): 303–371.
66. H. P. Chaliki, R. A. Nishimura, and M. Enriquez-Sarano, "A Simplified, Practical Approach to Assessment of Severity of Mitral Regurgitation by Doppler Color Flow Imaging With Proximal Convergence: Validation With Concomitant Cardiac Catheterization," *Mayo Clinic Proceedings* 73 (1998): 929–935.
67. C. Tribouilloy, W. F. Shen, J. L. Rey, et al., "Mitral to Aortic Velocity Time Integral Ratio. A Non-Geometric Pulsed-Doppler Regurgitant Index in Iso-rgitant Index in Iso-lated Pure Mitral Regurgitation," *European Heart Journal* 15 (1994): 1335–1339.
68. B. J. Roberts and P. A. Grayburn, "Color Flow Imaging of the Vena Contracta in Mitral Regurgitation: Technical Considerations," *Journal of the American Society of Echocardiography* 16 (2003): 1002–1006.
69. M. Enriquez-Sarano, F. A. Miller Jr, and S. N. Hayes, "Effective Mitral Regurgitant Orifice Area: Clinical Use and Pitfalls of the Proximal Isovelocity Surface Area Method," *Journal of the American College of Cardiology* 25 (1995): 703–709.
70. Y. Matsumura, S. Fukuda, H. Tran, et al., "Geometry of the Proximal Isovelocity Surface Area in Mitral Regurgitation by 3-Dimensional Color Doppler Echocardiography: Difference Between Functional Mitral Regurgitation and Prolapse Regurgitation," *American Heart Journal* 155 (2008): 231–238.
71. G. A. Cheimariotis, K. Haris, J. Lee, et al., "Flow Convergence Area Estimation on in Vitro Color Flow Doppler Images Using Deep Learning," in *Mediterranean Conference on Medical and Biological Engineering and Computing, IFMBE Proceedings*, Vol. 76 (Cham: Springer, 2019).
72. K. Tang, Z. Ge, R. Ling, et al., "Mitral Regurgitation Quantification From Multi-Channel Ultrasound Images via Deep Learning," in *Medical Image Computing and Computer Assisted Intervention (MICCAI)*, Vol. 14225 (Springer, Cham: Lecture Notes in Computer Science, 2023), 223–232.
73. Q. Zhang, Y. Liu, J. Mi, et al., "Automatic Assessment of Mitral Regurgitation Severity Using the Mask R-CNN Algorithm With Color Doppler Echocardiography Images," *Computational and Mathematical Methods in Medicine* 2021 (2021): 10.
74. F. Yang, X. Chen, X. Lin, et al., "Automated Analysis of Doppler Echocardiographic Videos as a Screening Tool for Valvular Heart Diseases," *JACC: Cardiovascular Imaging* 15, no. 4 (2022): 551–563.
75. M. Y. Elwazir, Z. Akkus, D. Oguz, et al., "Fully Automated Mitral Inflow Doppler Analysis Using Deep Learning," in *2020 Proceedings - IEEE 20th International Conference on Bioinformatics and Bioengineering (BIBE) (IEEE, 2020)*, 691–696.
76. S. H. Little, B. Pirat, R. Kumar, et al., "Three-Dimensional Color Doppler Echocardiography for Direct Measurement of Vena Contracta Area in Mitral Regurgitation: In Vitro Validation and Clinical Experience," *JACC: Cardiovascular Imaging* 1, no. 6 (2008): 695–704.
77. E. Hyodo, S. Iwata, A. Tugcu, et al., "Direct Measurement of Multiple Vena Contracta Areas for Assessing the Severity of Mitral Regurgitation Using 3D TEE," *JACC: Cardiovascular Imaging* 5 (2012): 669–766.
78. P. Thavendiranathan, D. Phelan, P. Collier, et al., "Quantitative Assessment of Mitral Regurgitation: How Best to Do It," *JACC: Cardiovascular Imaging* 5 (2012): 1161–1175.
79. F. Yang, X. Chen, X. Lin, et al., "Automated Analysis of Doppler Echocardiographic Videos as a Screening Tool for Valvular Heart Diseases," *JACC: Cardiovascular Imaging* 15 (2022): 551–563.
80. M. Shanks, H. M. Siebelink, V. Delgado, et al., "Quantitative Assessment of Mitral Regurgitation: Comparison Between Three-Dimensional Transesophageal Echocardiography and Magnetic Resonance Imaging," *Circulation: Cardiovascular Imaging* 3 (2010): 694–700.
81. X. Zeng, R. A. Levine, L. Hua, et al., "Diagnostic Value of vena Contracta Area in the Quantification of Mitral Regurgitation Severity by Color Doppler 3D Echocardiography," *Circulation: Cardiovascular Imaging* 4 (2011): 506–513.
82. G. Fiore, G. Ingallina, F. Ancona, et al., "Quantification of Mitral Regurgitation in Mitral Valve Prolapse by Three-Dimensional Vena Contracta Area: Derived Cutoff Values and Comparison With Two-Dimensional Multiparametric Approach," *Journal of the American Society of Echocardiography* 37, no. 6 (2024): 591–598.
83. J. Choi, R. Heo, G. R. Hong, et al., "Differential Effect of 3-Dimensional Color Doppler Echocardiography for the Quantification of Mitral Regurgitation According to the Severity and Characteristics," *Circulation: Cardiovascular Imaging* 7 (2014): 535–544.
84. P. Thavendiranathan, S. Liu, S. Datta, et al., "Quantification of Chronic Functional Mitral Regurgitation by Automated 3-Dimensional Peak and Integrated Proximal Isovelocity Surface Area and Stroke Volume Techniques Using Real-Time 3-Dimensional Volume Color Doppler Echocardiography: In Vitro and Clinical Validation," *Circulation: Cardiovascular Imaging* 6 (2013): 125–133.
85. W. Tsang, I. S. Salgo, D. Medvedofsky, et al., "Transthoracic 3D Echocardiographic Left Heart Chamber Quantification Using an Automated Adaptive Analytics Algorithm," *JACC: Cardiovascular Imaging* 9, no. 7 (2016): 769–782.
86. N. Brugger, K. Wustmann, M. Hurler, et al., "Comparison of Three-Dimensional Proximal Isovelocity Surface Area to Cardiac Magnetic Resonance Imaging for Quantifying Mitral Regurgitation," *American Journal of Cardiology* 115 (2015): 1130–1136.

87. R. A. Spampinato, F. Lindemann, C. Jahnke, et al., "Quantification of Regurgitation in Mitral Valve Prolapse With Automated Real Time Echocardiographic 3D Proximal Isovelocity Surface Area: Multimodality Consistency and Role of Eccentricity Index," *The International Journal of Cardiovascular Imaging* 37 (2021): 1947–1959.
88. S. Militaru, O. Bonnefous, K. Hami, et al., "Validation of Semi-automated Quantification of Mitral Valve Regurgitation by Three-Dimensional Color Doppler Transesophageal Echocardiography," *Journal of the American Society of Echocardiography* 33 (2020): 342–354.
89. F. C. Cobey, E. Ashihkmina, T. Edrich, et al., "The Mechanism of Mitral Regurgitation Influences the Temporal Dynamics of the Vena Contracta Area as Measured With Color Flow Doppler," *Anesthesia & Analgesia* 122 (2016): 321–329.
90. J. Hung, Y. Otsuji, M. D. Handschumacher, et al., "Mechanism of Dynamic Regurgitant Orifice Area Variation in Functional Mitral Regurgitation: Physiologic Insights From the Proximal Flow Convergence Technique," *Journal of the American College of Cardiology* 33 (1999): 538–545.
91. M. Enriquez-Sarano, L. J. Sinak, A. J. Tajik, et al., "Changes in Effective Regurgitant Orifice throughout Systole in Patients With Mitral Valve Prolapse. A Clinical Study Using the Proximal Isovelocity Surface Area Method," *Circulation* 92 (1995): 2951–2958.
92. A. Singh, J. Su, A. This, et al., "A Novel Approach for Semiautomated Three-Dimensional Quantification of Mitral Regurgitant Volume Reflects a More Physiologic Approach to Mitral Regurgitation," *Journal of the American Society of Echocardiography* 35, no. 9 (2022 Sep): 940–946.
93. R. M. Lang, L. P. Badano, V. Mor-Avi, et al., "Recommendations for Cardiac Chamber Quantification by Echocardiography in Adults: An Update From the American Society of Echocardiography and the European Association of Cardiovascular Imaging," *Journal of the American Society of Echocardiography* 28 (2015): 1–39.e14.
94. S. Marechaux, C. Le Goffic, P. V. Ennezat, et al., "Quantitative Assessment of Primary Mitral Regurgitation Using Left Ventricular Volumes: A Three-Dimensional Transthoracic Echocardiographic Pilot Study," *European Heart Journal – Cardiovascular Imaging* 15 (2014): 1133.
95. F. Levy, S. Marechaux, L. Iacuzio, et al., "Quantitative Assessment of Primary Mitral Regurgitation Using Left Ventricular Volumes Obtained With New Automated Three-Dimensional Transthoracic Echocardiographic Software: A Comparison With 3-Tesla Cardiac Magnetic Resonance," *Archives of Cardiovascular Diseases* 111, no. 8-9 (2018): 507–517.
96. V. Mor-Avi, C. Jenkins, H. P. Kühl, et al., "Real-Time 3-Dimensional Echocardiographic Quantification of Left Ventricular Volumes: Multicenter Study for Validation with Magnetic Resonance Imaging and Investigation of Sources of Error," *JACC: Cardiovascular Imaging* 1, no. 4 (2008): 413–423.
97. M. T. Nolan and P. Thavendiranathan, "Automated Quantification in Echocardiography," *JACC: Cardiovascular Imaging* 12 (2019): 1073–1092.
98. G. Tamborini, C. Piazzese, R. M. Lang, et al., "Feasibility and Accuracy of Automated Software for Transthoracic Three-Dimensional Left Ventricular Volume and Function Analysis: Comparisons With Two-Dimensional Echocardiography, Three-dimensional Transthoracic Manual Method, and Cardiac Magnetic Resonance Imaging," *Journal of the American Society of Echocardiography* 30, no. 11 (2017): 1049–1058.
99. F. M. Asch, N. Poilvert, T. Abraham, et al., "Automated Echocardiographic Quantification of Left Ventricular Ejection Fraction Without Volume Measurements Using a Machine Learning Algorithm Mimicking a human Expert," *Circulation: Cardiovascular Imaging* 12 (2019): e009303.
100. J. Verbeke, S. Calle, V. Kamoen, et al., "Prognostic Value of Myocardial Work and Global Longitudinal Strain in Patients With Heart Failure and Functional Mitral Regurgitation," *The International Journal of Cardiovascular Imaging* 38, no. 4 (2022): 803–812.
101. M. Cameli, G. E. Mandoli, D. Nistor, et al., "Left Heart Longitudinal Deformation Analysis in Mitral Regurgitation," *The International Journal of Cardiovascular Imaging* 34, no. 11 (2018): 1741–1751.
102. H. Ueyama, T. Kuno, H. Takagi, et al., "Prognostic Value of Left Ventricular Global Longitudinal Strain in Mitral Regurgitation: A Systematic Review," *Heart Failure Reviews* 28, no. 2 (2023): 465–483.
103. M. C. Meucci, J. Stassen, A. Tomsic, et al., "Prognostic Impact of Left Ventricular Global Longitudinal Strain in Atrial Mitral Regurgitation," *Heart* 109, no. 6 (2023): 478–484.
104. H. M. Kim, G. Y. Cho, I. C. Hwang, et al., "Myocardial Strain in Prediction of Outcomes After Surgery for Severe Mitral Regurgitation," *JACC: Cardiovascular Imaging* 11, no. 9 (2018): 1235–1244.
105. I. M. Salte, A. Østvik, E. Smistad, et al., "Artificial Intelligence for Automatic Measurement of Left Ventricular Strain in Echocardiography," *JACC: Cardiovascular Imaging* 14, no. 10 (2021): 1918–1928.
106. P. Barbier, O. Mirea, C. Cefalù, et al., "Reliability and Feasibility of Longitudinal AFI Global and Segmental Strain Compared With 2D Left Ventricular Volumes and Ejection Fraction: Intra- and Inter-Operator, Test–Retest, and Inter-Cycle Reproducibility," *European Heart Journal—Cardiovascular Imaging* 16, no. 6 (2015): 642–652.
107. A. Manovel, D. Dawson, B. Smith, et al., "Assessment of Left Ventricular Function by Different Speckle-Tracking Software," *European Journal of Echocardiography* 11, no. 5 (2010): 417–421.
108. K. C. Huang, C. S. Huang, M. Y. Su, et al., "Artificial Intelligence Aids Cardiac Image Quality Assessment for Improving Precision in Strain Measurements," *JACC: Cardiovascular Imaging* 14, no. 2 (2021): 335–345.
109. C. Knackstedt, S. Bekkers, G. Schummers, et al., "Fully Automated versus Standard Tracking of Left Ventricular Ejection Fraction and Longitudinal Strain: The FAST-EFs Multicenter Study," *Journal of the American College of Cardiology* 66, no. 13 (2015): 1456–1466.
110. D. A. Gomes, P. M. Lopes, P. Freitas, et al., "Peak Left Atrial Longitudinal Strain Is Associated With All-Cause Mortality in Patients With Ventricular Functional Mitral Regurgitation," *Cardiovascular Ultrasound* 21 (2023): 9.
111. M. Cameli, M. C. Pastore, F. M. Righini, et al., "Prognostic Value of Left Atrial Strain in Patients With Moderate Asymptomatic Mitral Regurgitation," *The International Journal of Cardiovascular Imaging* 35, no. 9 (2019): 1597–1604.
112. N. Ajmone Marsan, V. Delgado, D. J. Shah, et al., "Valvular Heart Disease: Shifting the Focus to the Myocardium," *European Heart Journal* 44, no. 1 (2023): 28–40.
113. Y. Ye, R. Desai, L. M. Vargab Abello, et al., "Effects of Right Ventricular Morphology and Function on Outcomes of Patients With Degenerative Mitral Valve Disease," *Journal of Thoracic and Cardiovascular Surgery* 148 (2014): 2012–2020.
114. L. Lupi, L. Italia, M. Pagnesi, et al., "Prognostic Value of Right Ventricular Longitudinal Strain in Patients With Secondary Mitral Regurgitation Undergoing Transcatheter Edge-to-Edge Mitral Valve Repair," *European Heart Journal—Cardiovascular Imaging* 24, no. 11 (2023): 1509–1517.
115. D. Medvedofsky, K. Addetia, A. R. Patel, et al., "Novel Approach to Three-Dimensional Echocardiographic Quantification of Right Ventricular Volumes and Function From Focused Views," *Journal of the American Society of Echocardiography* 28, no. 10 (2015): 1222–1231.
116. M. C. Pastore, G. E. Mandoli, H. S. Aboumarie, et al., "Basic and Advanced Echocardiography in Advanced Heart Failure: An Overview," *Heart Failure Reviews* 25 (2019): 937–948.
117. M. Tadic, N. Nita, L. Schneider, et al., "The Predictive Value of Right Ventricular Longitudinal Strain in Pulmonary Hypertension, Heart Failure, and Valvular Diseases," *Frontiers in Cardiovascular Medicine* 8 (2021): 698158.